

# Diagnostic Tests for Nested Sampling Calculations

Edward Higson<sup>\*,1,2</sup>, Will Handley<sup>1,2</sup>, Mike Hobson<sup>1</sup>, Anthony Lasenby<sup>1,2</sup>

<sup>1</sup>Cavendish Astrophysics Group, University of Cambridge,  
Cambridge, UK, CB3 0HE

<sup>2</sup>Kavli Institute for Cosmology, University of Cambridge,  
Cambridge, UK, CB3 0HA

September 2, 2022

## Abstract

Nested sampling is an increasingly popular technique for Bayesian computation — in particular for multimodal, degenerate and high-dimensional problems. Without appropriate settings, however, nested sampling software may fail to explore such posteriors fully; for example producing correlated samples or missing significant modes. This paper introduces new diagnostic tests to assess the reliability of both parameter estimation and evidence calculations using nested sampling software, and demonstrates them empirically. We present two new diagnostic plots for nested sampling, and give practical advice for nested sampling software users. Our diagnostic tests and diagrams are implemented in **nestcheck**<sup>1</sup>: a publicly available python package for analysing nested sampling calculations which is compatible with results from MULTINEST and POLYCHORD.

*Keywords:* statistical computing, measurement error, software, bootstrap/resampling, Bayesian methods

## 1 Introduction

Nested sampling (Skilling 2006) is a method for Bayesian analysis which simultaneously provides Bayesian evidences and posterior samples. Though nested sampling was originally designed for evidence calculation, the popular MULTINEST (Feroz & Hobson 2008, Feroz

---

<sup>\*</sup>e.higson@mrao.cam.ac.uk

<sup>1</sup>Available at <https://github.com/ejhigson/nestcheck>; see the documentation for more details.

et al. 2008, 2013) and POLYCHORD (Handley et al. 2015*a,b*) implementations are now used extensively for parameter estimation. Nested sampling performs well compared to Markov chain Monte Carlo (MCMC)-based alternatives for parameter estimation of high-dimensional, degenerate and multimodal posteriors as it has no thermal transition property and does not require the specification of a proposal function.

Uncertainty in results due to the stochasticity of the nested sampling algorithm can be estimated numerically for parameter estimation (Higson et al. 2017*b*) and evidence calculations (Skilling 2006, Keeton 2011). However all of these techniques assume that the nested sampling algorithm was executed perfectly, which requires sampling randomly from the prior within a hard likelihood constraint. Nested sampling software used for practical problems can only do this approximately and, as a result, may produce additional errors; for example from correlated samples or missing parts of the posterior. We term these additional errors *implementation-specific effects* to distinguish them from the intrinsic stochasticity of the nested sampling algorithm. Typically software has settings which reduce implementation-specific effects but increase computational cost, such as POLYCHORD’s `num.repeats` and MULTINEST’s `efr`. Depending on the problem considered and the software and settings used, implementation-specific effects can be very large — for example if the algorithm misses a significant mode in a multimodal posterior.

Diagnosing whether significant implementation-specific effects are present is of great practical importance, as users may need to adjust the software settings to achieve reliable results (see Section 5.1 for more details). In contrast, if implementation-specific effects are negligible then users can simply increase the number of live points for more accurate results, and can confidently use standard techniques to estimate numerical uncertainty from the nested sampling algorithm.

Software users typically try to check if the algorithm has explored the posterior correctly by running a calculation several times and qualitatively assessing if the posterior distributions look similar in each case. However this is not very reliable and does not differentiate between implementation-specific effects and the expected variation from the inherent stochasticity of the nested sampling algorithm. We are not aware of any diagnostic tests in the literature for checking calculation results for practical problems for implementation-specific effects (Buchner (2016) proposes a diagnostic which uses analytically solvable test problems). In contrast, Markov chain Monte Carlo (MCMC)-based methods, which do not require sampling within a hard likelihood constraint, have an extensive literature on diagnostics for practical problems (see for example Hogg & Foreman-Mackey 2017).

This paper introduces new heuristic tests and diagrams to check the reliability of nested sampling results for practical problems, and to determine if the software settings should be changed. It is also intended to serve as a practical guide for nested sampling practitioners based on the authors’ experience using nested sampling software. We begin with a brief background on the nested sampling algorithm and its associated errors in Section 2, and introduce some test problems in Section 3 which we use to illustrate our discussion throughout. Section 4 discusses diagnostic plots and presents two new diagrams for nested sampling (illustrated in Figures 3 to 5). Section 5 describes how the implementation-specific effects can be measured from a set of nested sampling runs. We empirically test the effects of changing nested sampling software settings both on implementation-specific effects and to-

tal calculation errors using POLYCHORD in Section 5.1. Finally, in Section 6 we introduce quantitative diagnostic tests to check for implementation-specific effects which can be used when as few as 2 nested sampling runs are available.

## 2 Background: nested sampling and sampling errors

This section provides a brief overview of the nested sampling algorithm and the sampling errors involved in the process — for more details see Higson et al. (2017b). A comparison of nested sampling with other sampling methods is beyond of the scope of this paper; for this we refer the reader to Allison & Dunkley (2014) and Murray (2007).

Nested sampling (Skilling 2006) performs Bayesian computations by maintaining a set of samples from the prior  $\pi(\theta)$ , called *live points*, and repeatedly replacing the point with the lowest likelihood  $\mathcal{L}(\theta)$  with another sample from the region of the prior with a higher likelihood. The samples which have been removed, termed *dead points*, are then used for evidence calculations and posterior inferences (the live points remaining when the algorithm terminates can also be included). The fraction of the prior volume remaining after each point  $i$  with likelihood  $\mathcal{L}_i$ , which we define as

$$X(\mathcal{L}_i) \equiv \int_{\mathcal{L}(\theta) > \mathcal{L}_i} \pi(\theta) d\theta, \quad (1)$$

shrinks exponentially; this process is illustrated schematically in Figure 1. The shrinkage at each step is unknown but is estimated statistically and used to weight the samples produced. The accuracy of results can be greatly improved — in particular for high-dimensional parameter estimation problems — by using dynamic nested sampling (Higson et al. 2017a), in which the number of live points varies to allocate samples more efficiently.

The sampling errors from this process can be estimated by dividing a completed nested sampling run with some number of live points into many valid nested sampling runs with only one live point. These single live point runs, termed *threads*, can then be resampled using standard techniques such as the bootstrap as described in Section 4 of Higson et al. (2017b). The resampling is valid as the log  $X$  values of the dead points of a nested sampling run with  $n$  live points are a Poisson process with rate  $n$ , so hence the log  $X$  values for the dead points in each of its constituent threads form a Poisson process of rate 1.

## 3 Test problems

We now introduce four test problems which pose different challenges for nested sampling software, and which will be used for numerical tests in the remainder of this paper.

For comparison with more complex likelihoods we first use the simple  $d$ -dimensional Gaussian likelihood centred on the origin

$$\log \mathcal{L}(\theta) = -\frac{d}{2} \log(2\pi) - \frac{|\theta|^2}{2\sigma^2}, \text{ where for our tests we set } \sigma = 0.5. \quad (2)$$

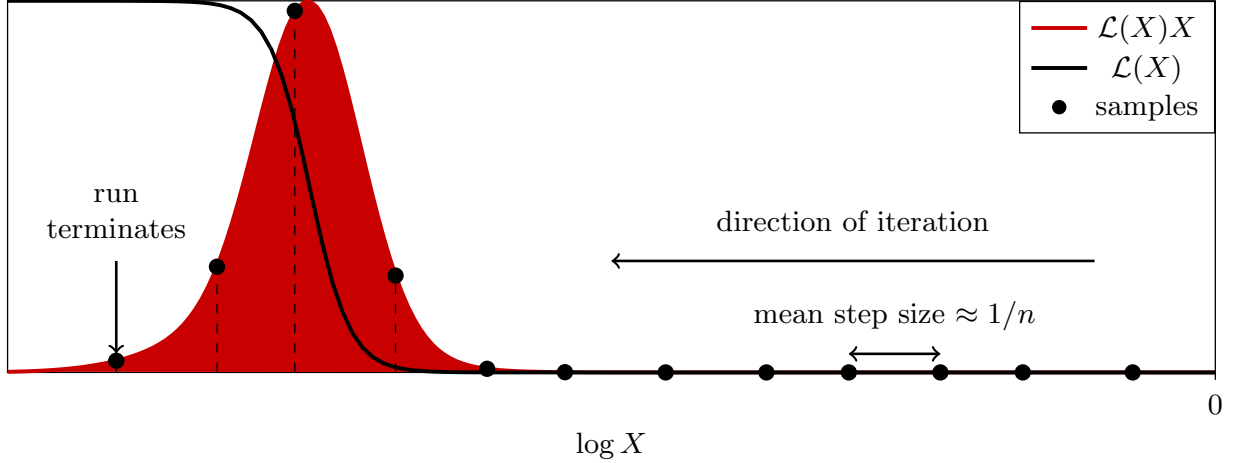


Figure 1: Illustration of nested sampling with a constant number of live points  $n$  (reproduced from Higson et al. 2017b). The algorithm samples an exponentially shrinking fraction of the prior  $X$  as it moves towards increasing likelihoods. The relative posterior mass contained at each  $\log X$  value is proportional to  $\mathcal{L}(X)X$ , where  $\mathcal{L}(X) \equiv X^{-1}(\mathcal{L})$ .

A more challenging case is the Gaussian shell likelihood centred on the origin with radius  $r$  and width  $w$

$$\log \mathcal{L}(\theta) = C_{\text{GS}} - \frac{(|\theta| - r)^2}{2w^2} \text{ where we will use } r = 2, w = 0.1, \quad (3)$$

and  $C_{\text{GS}}$  is a normalisation constant. As an example of a highly multimodal likelihood we use the  $d$ -dimension Rastrigin function

$$\log \mathcal{L}(\theta) = C_{\text{Ra}} - \sum_{i=1}^n (\theta_i^2 - 10 \cos(2\pi\theta_i)), \quad (4)$$

where  $\theta_i$  is the  $i^{\text{th}}$  component of the parameter vector  $\theta$  and  $C_{\text{Ra}}$  is a normalisation constant. This is the industry standard “bunch of grapes” and exploring it correctly requires algorithms not to become stuck in local maxima or miss modes containing significant posterior mass. Finally we consider the  $d$ -dimensional Rosenbrock function (industry standard “banana”)

$$\log \mathcal{L}(\theta) = C_{\text{Ro}} - \sum_{i=1}^{n-1} \left( (a - \theta_i)^2 + b(\theta_{i+1} - \theta_i^2)^2 \right) \text{ where we use } a = 1, b = 100, \quad (5)$$

which has a long, curving degeneracy. Our numerical tests all use uniform priors  $\in [-10, 10]$  for each parameter.

We use 2-dimensional likelihoods and priors to perform nested sampling calculations many times and measure the variation of results, with software settings chosen to illustrate implementation-specific effects. Higher dimension problems do not change our analysis or conclusions but require more computational effort; for example computational costs with

MULTINEST increase exponentially with the dimension  $d$  and with POLYCHORD scale as  $\sim \mathcal{O}(d^3)$  (Handley et al. 2015b). Our diagnostic tests are particularly useful for checking results when taking significantly more samples is computationally costly, as is often the case for high-dimensional problems.

For simplicity we use a constant number of live points for numerical tests in this paper, but our analysis also applies to dynamic nested sampling (Higson et al. 2017a) in which the number of live points is allowed to vary.

## 4 Diagnostic plots

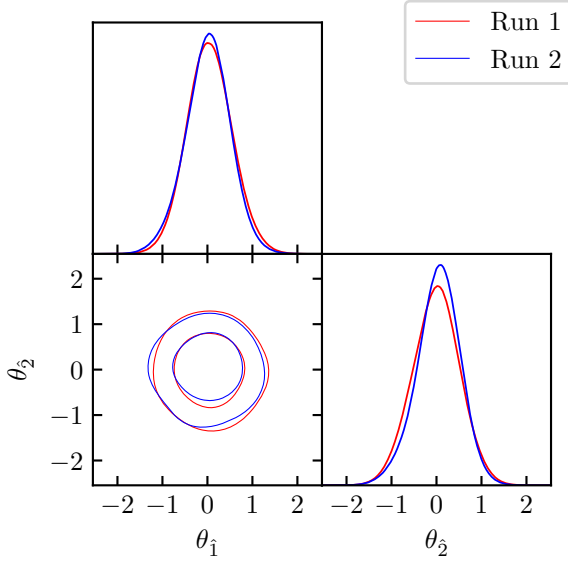
Before discussing quantitative diagnostics in Sections 5 and 6, we first introduce some diagnostic plots which illustrate nested sampling and its associated errors. It is good practice for users of sampling software to represent their results visually, in order to assess if they are reasonable given background knowledge about the problem being considered. Many software packages exist for plotting 1- and 2-dimensional marginalised distributions from weighted samples using kernel density estimation; see for example Foreman-Mackey (2016), Lewis (2015). Figures 2a to 2d show posterior distributions calculated from POLYCHORD nested sampling runs for 2-dimensional Gaussian (2), Gaussian shell (3), Rastrigin (4) and Rosenbrock (5) likelihoods with uniform priors, made using the `getdist` package.

While plots like Figures 2a to 2d are useful, it is unclear to what extent the differences between the two nested sampling runs are due to implementation-specific effects or merely what is expected from the stochasticity of the nested sampling algorithm. In addition, these plots are generic for all methods of sampling and do not adequately represent the distinctive manner in which nested sampling iterates towards higher likelihoods. We therefore propose two additional diagnostic plots which can be calculated from nested sampling runs in Sections 4.1 and 4.2 to illustrate this extra information.

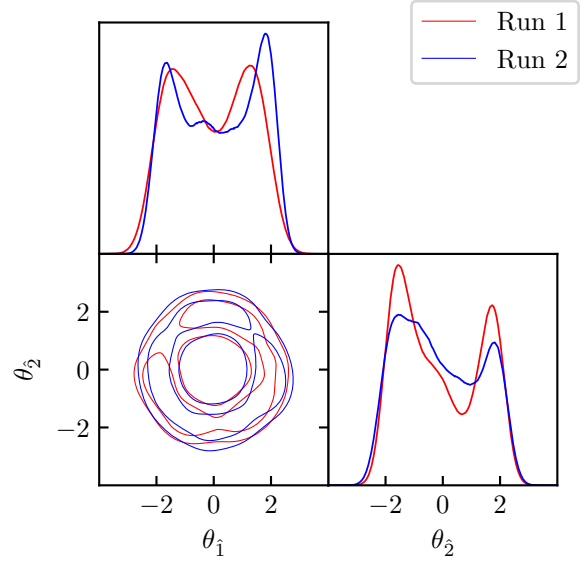
### 4.1 Uncertainty on posterior distributions

The error on calculated posterior distributions due to nested sampling stochasticity can be estimated using bootstrap resamples of the run (as described in Higson et al. 2017b). This uncertainty can be visually represented by plotting the distribution of the posteriors from resampled runs to give an *uncertainty distribution on the posterior distribution*. Such plots can be used for assessing if the uncertainty is sufficiently small for the given use case, and are illustrated in Figures 3a to 3d.

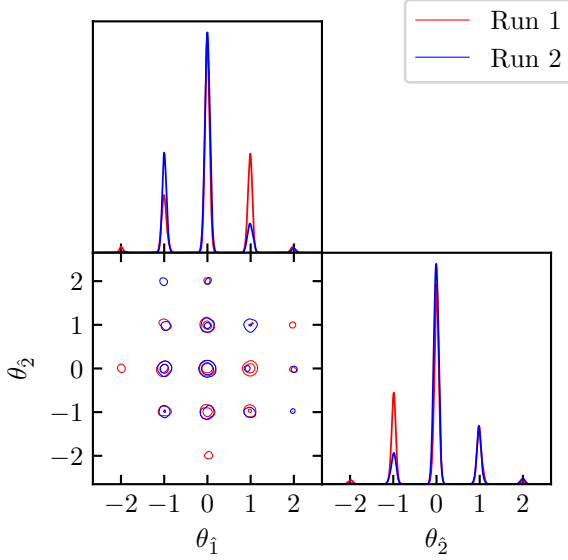
Plotting multiple runs on the same axis allows visual assessment of whether implementation-specific effects are present. If posterior distributions differ by more than would be expected from their bootstrap sampling error distribution, then implementation-specific effects are likely to be the cause. This is the case for the runs shown in Figures 3c and 3d and suggest relatively large implementation-specific effects may be present in these cases with the settings used, whereas the differences between runs in Figures 3a and 3b are within the range that might be expected given the stochasticity of the nested sampling algorithm. These plots use the POLYCHORD setting `num.repeats` = 5 which is deliberately chosen to illus-



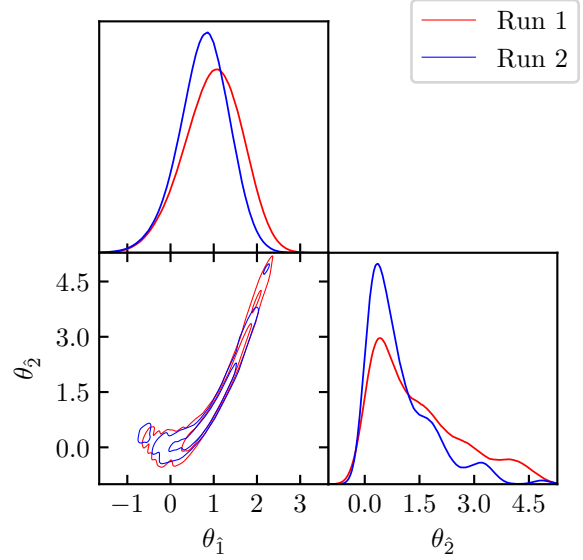
(a) 2-dimensional Gaussian likelihood (2).



(b) 2-dimensional Gaussian shell likelihood (3).



(c) 2-dimensional Rastrigin likelihood (4).



(d) 2-dimensional Rosenbrock likelihood (5).

Figure 2: Triangle plots for 2 nested sampling runs (red and blue lines) calculated using POLYCHORD and plotted using `getdist`. In each subfigure the top and right plots show 1-dimensional marginalised posterior distributions on the two parameters  $\theta_1$  and  $\theta_2$ , and the bottom left plot shows calculated 2-dimensional 68% and 95% credible intervals on the joint posterior distribution. The results for the two runs differ due to errors from both the intrinsic stochasticity of the nested sampling algorithm and implementation-specific effects. Each nested sampling run has 100 live points and uses the POLYCHORD setting `num_repeats` = 5 — these are deliberately chosen to make the errors big enough to be easily visible in the plots. Reducing errors by changing the calculation settings is discussed in Section 5.1.

trate the implementation-specific effects; they can be reduced by increasing `num_repeats` as discussed in Section 5.1.

When calculating plots like Figures 3a to 3d, the posterior distribution for each bootstrap replication must be calculated from the weighted samples without reducing them to evenly weighted samples in a stochastic manner — such as by including each sample with probability proportional to its weight — as this adds extra variation. `nestcheck` contains an implementation of 1-dimensional kernel density estimation which takes sample weights as an argument, and does not require conversion to evenly weighted samples.

## 4.2 Distributions of samples in $\log X$

For an insight into how nested sampling software explores a parameter space, we recommend plotting diagrams based on the representation of nested sampling parameter estimation in terms of  $\log X$  discussed in Higson et al. (2017b, Figure 3), where  $X$  is defined in (1). By plotting samples’ parameter values against their estimated  $\log X$  coordinate one may visualise the distribution of parameters in the region of each iso-likelihood contour  $\mathcal{L}(\theta) = \mathcal{L}(X)$  and see where in the sampling process modes separate from each other.

Our proposed diagram for analysing nested sampling software output is illustrated in Figures 4a, 4b, 5a and 5b. In each case the top right panel is similar to Figure 1 and shows the calculated relative posterior mass (total weight assigned to all samples in that region) at each  $\log X$  value, as well as its uncertainty distribution from the stochasticity of the nested sampling algorithm. Each subsequent row represents a parameter or function of parameters; the right panel plots sampled values against  $\log X$  and the left panel shows its posterior distribution in the same way as Figures 3a to 3d. As nested sampling estimates points’  $\log X$  positions statistically, the  $x$ -coordinates of the posterior samples on the scatter plots are only approximate and include stochastic errors. The evolution of individual threads can be traced by drawing lines linking their constituent points. This shares similarities with MCMC trace plots but, unlike for a converged MCMC chain, the distribution of parameters typically changes as the algorithm iterates over different  $\log X$  values. Plots which trace individual threads in  $\log X$  are also produced by the `dynesty`<sup>2</sup> dynamic nested sampling package.

Figures 4a, 4b, 5a and 5b are useful for visualising the nested sampling process and parts of the posterior such as degeneracies and modes with which nested sampling software may struggle. For example Figure 5a clearly shows the multi-modality of the Rastrigin likelihood, as well as giving in indication of how far into the nested sampling process the modes separate. This contrasts with the bottom right panels of Figures 4a and 4b, which show that the radial coordinate  $|\theta|$  has very little spread at any given  $\log X$  value in these cases (due to the likelihoods’ spherical symmetry). Furthermore, if problem-specific knowledge about the expected distributions of parameters is available, this type of diagram can be useful in working out where the sampler is not behaving as expected as well as in diagnosing problems.

In addition, multiple nested sampling runs can be added to the same axis, as shown in Figures 5a and 5b. This allows comparison of where runs differ; for example if one of the

<sup>2</sup><https://github.com/joshspeagle/dynesty>.

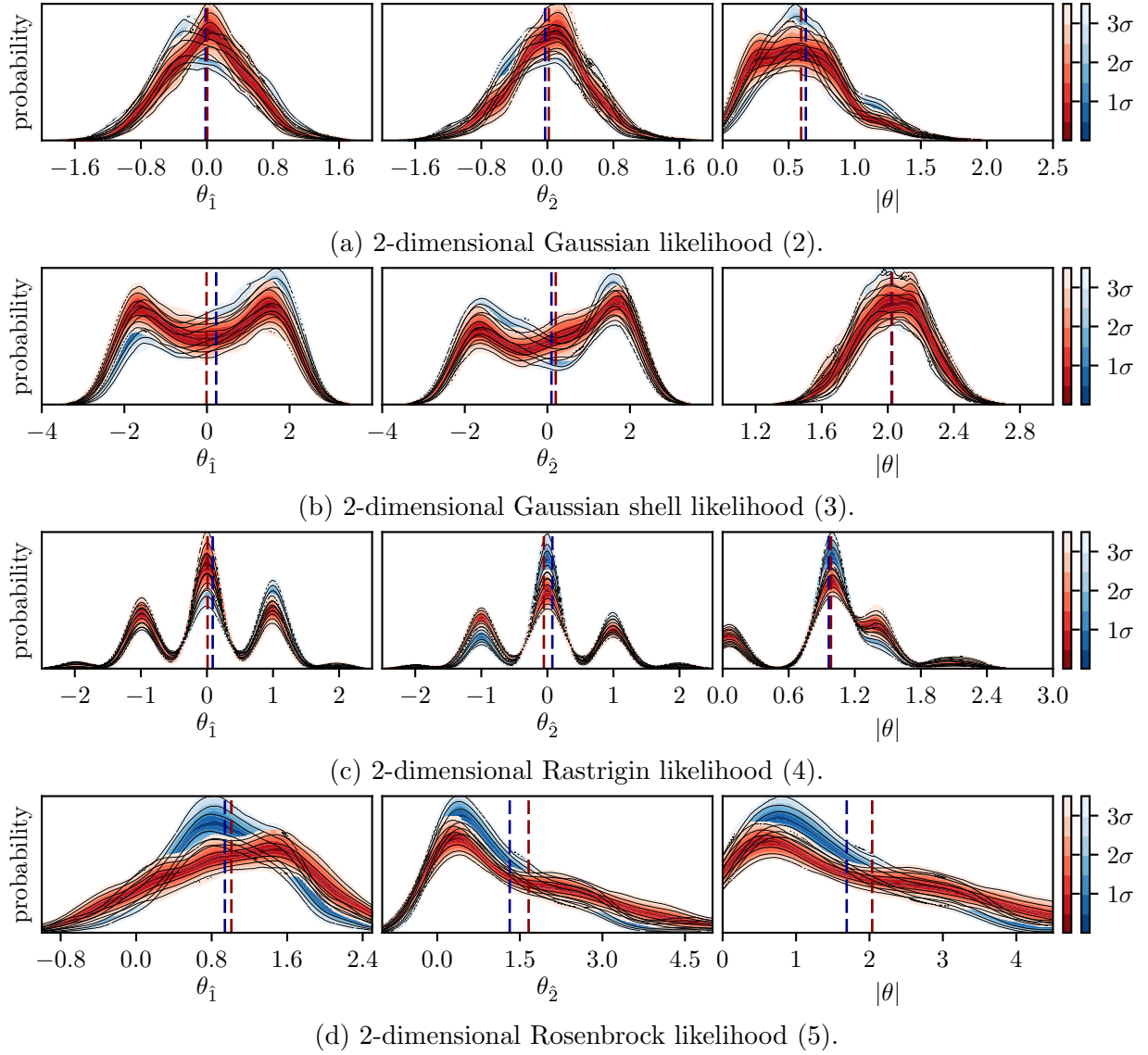


Figure 3: Diagrams of posterior distributions of parameters, produced with `nestcheck`, for the two nested sampling runs (red and blue) used in each of Figures 2a to 2d. Colours show the uncertainty on the distribution from the stochasticity of the nested sampling algorithm, calculated by bootstrap resampling the run. For each likelihood sub-figure, the first two plots show the posterior distributions on parameters  $\theta_1$  and  $\theta_2$ , and can be compared to the similar 1-dimensional plots in Figures 2a to 2d. The right-most plots show the posterior distribution on the radial coordinate  $|\theta| = \sqrt{\theta_1^2 + \theta_2^2}$  and illustrate how posterior distributions of functions of parameters can also be plotted. The dashed dark blue and dark red lines show the estimated posterior means of each parameter for the blue and red runs respectively. The coloured contours show iso-probability credible intervals on the marginalised posterior probability density function at each parameter value.



runs shown in Figure 5a had missed a mode which the other run found, it would be easily visible in the plot. One can also see from Figure 5b that the two runs agree closely on the relative weights assigned at different  $\log X$  values (top panel), meaning that the difference between the posterior distributions (left panels) is due to the parameter values sampled in each  $\log X$  region rather than the regions’ relative weights.

The scatter plots in the right column of Figures 4a, 4b, 5a and 5b can be replaced with a colour plot of the estimated distribution of values at each  $\log X$  using kernel density estimation (similar to the colour distributions shown in Figure 3 of Higson et al. 2017b). However doing this accurately is computationally challenging and requires a lot of samples, so simple scatter plots are typically more convenient for checking calculation results.

## 5 Measuring implementation-specific effects

Following the diagnostics plots of the previous section, the remainder of this paper discusses quantitatively measuring implementation-specific effects. The total error on nested sampling calculations can be estimated by measuring the variation of results when a calculation is repeated multiple times, as this includes both implementation-specific effects and the intrinsic stochasticity of the algorithm. This may be an underestimate if most or all of the calculations miss some part of the posterior — for example a very difficult to locate mode containing significant posterior mass. However for the cases we consider in this paper we find empirically that the standard deviation of results is typically very close to root-mean-squared error, even when significant implementation-specific effects are present.

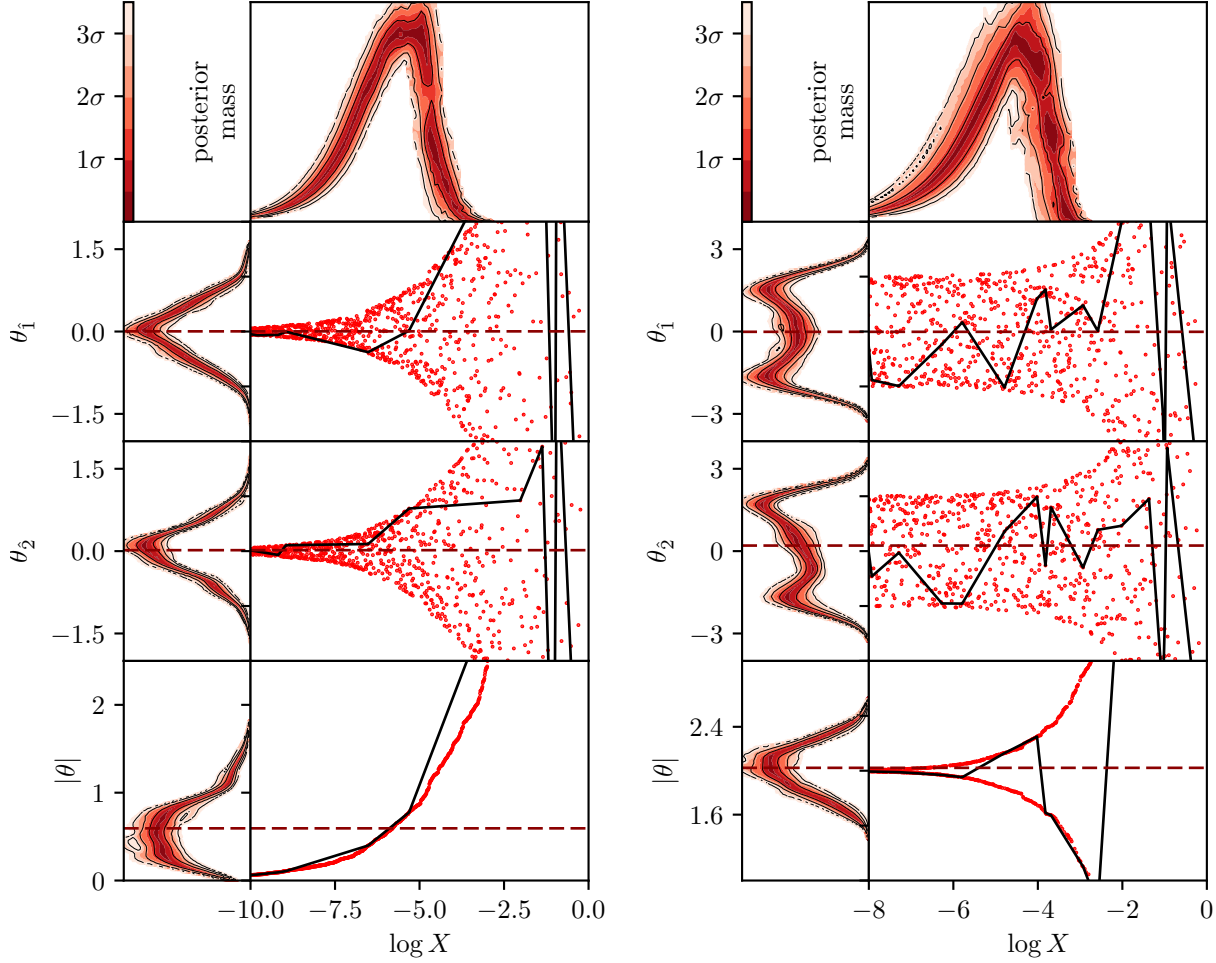
While the nature of implementation-specific effects depends on the specific software used, they are very likely to be uncorrelated with the errors from the stochasticity of the nested sampling algorithm — which can be calculated using the bootstrap resampling approach described in Higson et al. (2017b). As a result, the implementation-specific effects are related to the sample standard deviation of calculation results  $\sigma_{\text{values}}$  and the mean bootstrap sampling error estimate  $\sigma_{\text{bootstrap}}$  by

$$\sigma_{\text{values}}^2 \approx \sigma_{\text{bootstrap}}^2 + \sigma_{\text{implementation}}^2, \quad (6)$$

and the standard deviation of the uncertainty distribution due to implementation-specific effects can be estimated as

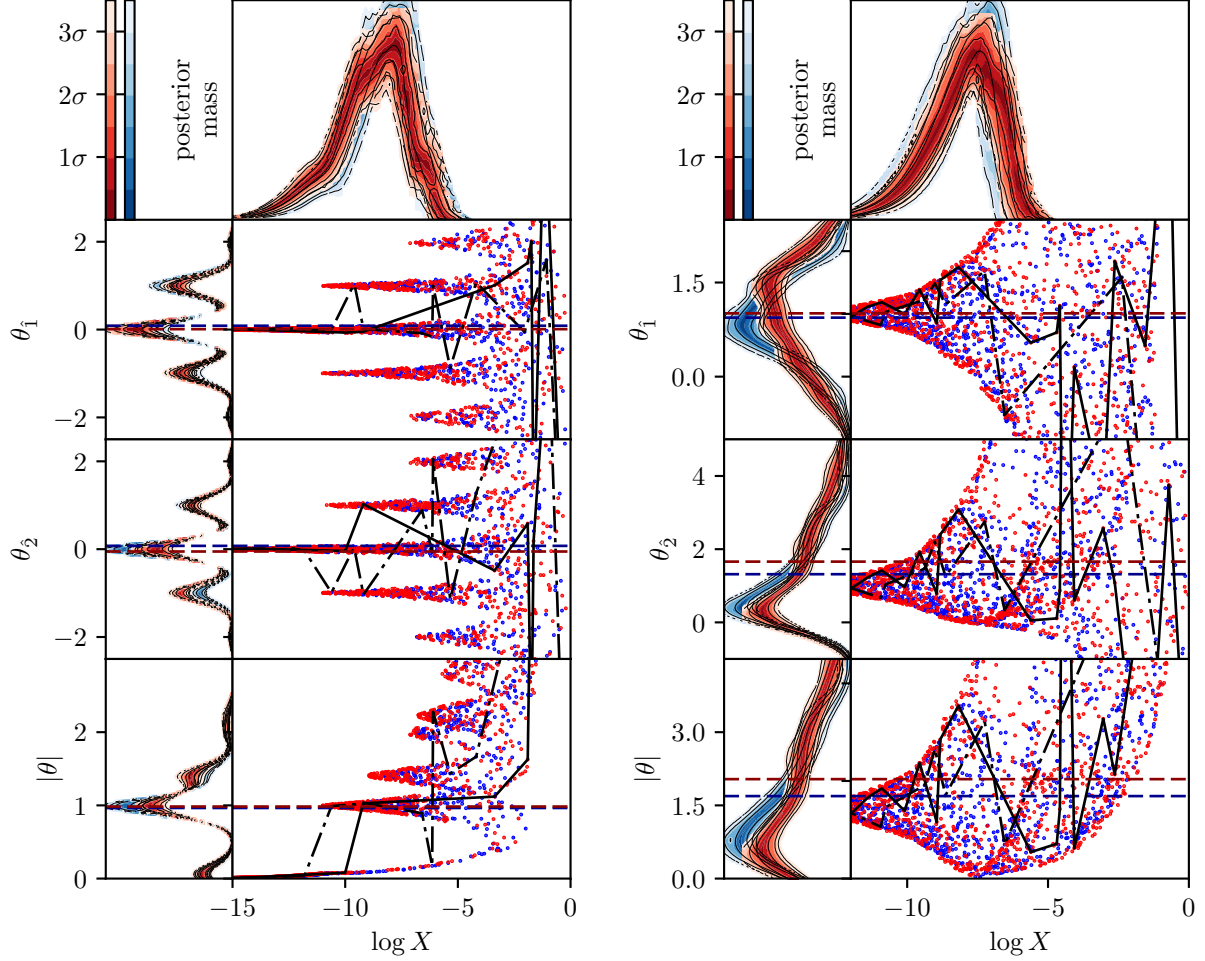
$$\sigma_{\text{implementation}} \approx \begin{cases} \sqrt{\sigma_{\text{values}}^2 - \sigma_{\text{bootstrap}}^2} & \text{if } \sigma_{\text{values}}^2 > \sigma_{\text{bootstrap}}^2, \\ 0 & \text{otherwise.} \end{cases} \quad (7)$$

If a number of nested sampling runs are available, the implementation-specific effects on calculations of scalar quantities such as the mean and median of parameters can be calculated directly from (7) and compared to the variation of results. One can also estimate the fraction of the observed variation which is due to implementation-specific effects  $\sigma_{\text{implementation}}/\sigma_{\text{values}}$  — when implementation-specific effects are large this is easy to measure accurately as the variation of results is much greater than the bootstrap error estimates



(a) 2-dimensional Gaussian likelihood (2). (b) 2-dimensional Gaussian shell likelihood (3).

Figure 4: Diagrams of samples' distributions in  $\log X$  produced using `nestcheck`. The nested sampling runs shown use 100 live points and `num.repeats` = 5. The top right panel shows the relative posterior mass (total weight assigned to all samples in that region) at each  $\log X$  value. Each subsequent row represents a parameter or function of parameters, and in each the right panel plots its sampled values against  $\log X$  and the left panel shows its posterior distribution in the same way as Figures 3a and 3b. The solid black lines show the evolution of an individual thread from each run (chosen at random). The estimated mean value of the parameter or function of parameters from the run is marked with a dashed line. The coloured contours show iso-probability credible intervals on the marginalised posterior probability density function at each parameter or  $\log X$  value.



(a) 2-dimensional Rastrigin likelihood (4).

(b) 2-dimensional Rosenbrock likelihood (5).

Figure 5: As for Figure 4 but using different likelihoods and showing two nested sampling runs plotted on the same axis. The nested sampling runs shown in red and blue are the same ones used for Figures 2c and 2d and Figures 3c and 3d. The dashed dark blue and dark red lines show the estimated posterior means of each parameter for the blue and red runs respectively. The solid and dot dash black lines show the evolution of an individual thread chosen at random from the red and blue runs respectively.

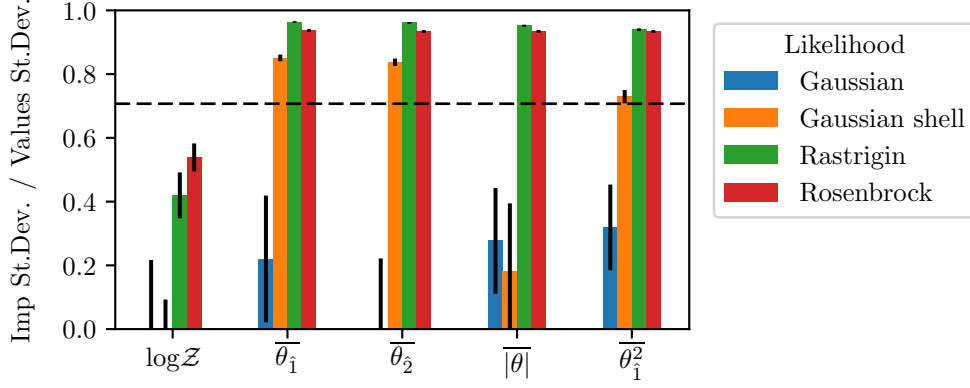


Figure 6: Ratios of estimated implementation-specific effects (7) to variation of results for 2-dimensional Gaussian (2), Gaussian shell (3), Rastrigin (4) and Rosenbrock (5) likelihoods with uniform priors. Equal contributions to the total error from implementation-specific effects and bootstrap errors gives a ratio of  $\frac{1}{\sqrt{2}}$  (not  $\frac{1}{2}$ ) from (7) — this is marked by the dashed horizontal line. Each bar is calculated using 500 POLYCHORD runs, each with 100 live points and `num_repeats` = 5; these settings are deliberately chosen to illustrate implementation-specific effects. Results are shown for the log-evidence, the mean of the two parameters, the mean radial coordinate and the second moment of  $\theta_1$ . The numerical results plotted in this figure are given in Tables 1 to 4 in Section B of the supplementary material.

and

$$\frac{\sigma_{\text{implementation}}}{\sigma_{\text{values}}} \approx \frac{\sqrt{\sigma_{\text{values}}^2 - \sigma_{\text{bootstrap}}^2}}{\sigma_{\text{values}}} = 1 - \frac{\sigma_{\text{bootstrap}}}{2\sigma_{\text{values}}} + \mathcal{O}\left(\frac{\sigma_{\text{bootstrap}}^2}{\sigma_{\text{values}}^2}\right). \quad (8)$$

We find empirically that  $\sim 8$  or more runs is enough to get a reasonable indication of whether large implementation-specific effects are present using (7) and (8).

Figure 6 shows the ratio of the inferred implementation error to the total variation of results for 500 nested sampling runs using 2-dimensional Gaussian (2), Gaussian shell (3), Rastrigin (4) and Rosenbrock (5) likelihoods. As for Figures 2 to 5 we use low values for the number of live points and POLYCHORD’s `num_repeats` setting in order to illustrate implementation-specific effects using 2-dimensional calculations. The numerical results plotted in Figure 6 are given in Tables 1 to 4 in Section B of the supplementary material, along with the absolute values of the variation of results, root-mean-squared errors and implementation error estimates. With these POLYCHORD settings implementation-specific effects dominate parameter estimation for the Rastrigin and Rosenbrock cases, and are also significant for the Gaussian shell likelihood in some parameter estimation quantities. However, the implementation fraction of the error for the log-evidence calculations is significantly lower than for parameter estimation; this is largely because errors from the stochasticity of the nested sampling algorithm are much larger for evidence calculation than for parameter estimation.

## 5.1 Effects of software settings on errors

We now empirically test the effect of software settings on the total error and the implementation error in calculations using POLYCHORD.

Nested sampling software typically has settings controlling the process of sampling within a hard likelihood constraint which are specific to a given package and can reduce implementation-specific effects at the cost of increased computation. POLYCHORD’s `num_repeats` setting controls the number of slice samples taken before sampling each new live point — the higher this is set the lower the correlation between points and the more accurately POLYCHORD will perform the nested sampling algorithm. Other examples of similar parameters include MULTINEST’s `efr`, which controls the efficiency of its rejection sampling algorithm by determining the size of the ellipsoid within which MULTINEST samples. If `efr` is lowered, samples are drawn from a larger ellipsoid, increasing the rejection rate whilst consequently decreasing the chance of missing part of the parameter space within the iso-likelihood contour.

Figure 7 shows the effect on calculation errors of POLYCHORD’s `num_repeats` setting. As expected, we see that as `num_repeats` is increased the implementation-specific effects fall and the variation of calculation results converges with the bootstrap error estimate, showing POLYCHORD is performing the nested sampling algorithm with increasing accuracy. The `num_repeats` value required for implementation-specific effects to be smaller than the bootstrap error estimates is several orders of magnitude higher for the Rastrigin and Rosenbrock likelihoods than for the simple Gaussian likelihood, illustrating the importance of implementation-specific effects for degenerate and multimodal posteriors.

In addition to software specific settings, the main choice a nested sampling user must make is the number of live points, which controls the resolution of sampling and is proportional to the expected number of dead points produced. For simplicity we consider only standard nested sampling, which uses a constant number of live points  $n$ , although our conclusions also apply to dynamic nested sampling (Higson et al. 2017a) where the local number of live points varies to increase calculation accuracy. The change in calculation errors with  $n$  is shown in Figure 8. As expected, increasing the live points reduces the implementation-specific effects, as well as the errors from the stochasticity of the nested sampling algorithm (measured by bootstrap resampling) which are approximately proportional to  $1/\sqrt{n}$ . The fraction of the total error made up by implementation-specific effects does not necessarily decrease with increased  $n$  — this depends on how the implementation-specific effects scale with  $n$ . For the Gaussian likelihood implementation-specific effects cause only a small part of the total variation of results, whereas for the more challenging Rastrigin and Rosenbrock likelihoods they are the main source of errors.

Given that increasing  $n$  reduces both implementation-specific effects and errors from the stochasticity of the nested sampling algorithm, this is often a better way to reduce total errors for the same computational cost than increasing `num_repeats`. In particular, in the Rastrigin and Rosenbrock cases there are diminishing returns of increasing `num_repeats` to very high values as can be seen in Figure 7. However while increasing  $n$  may make the absolute errors small enough for the given use case, it is not guaranteed to reduce the fraction of errors from implementation-specific effects; as a result techniques for estimating

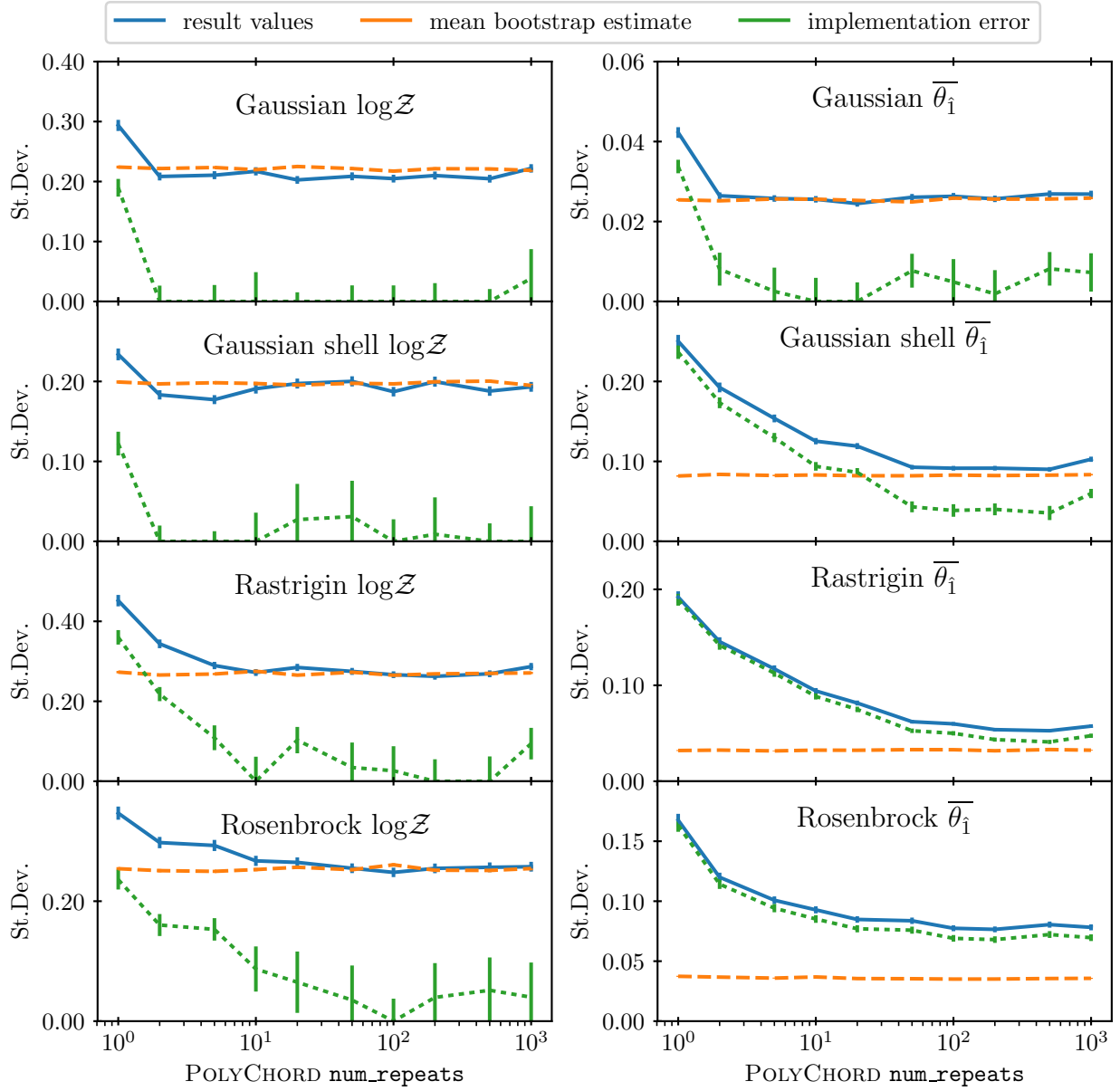


Figure 7: The effect of POLYCHORD’s `num_repeats` setting on results errors: blue solid lines show the standard deviation of repeated calculation results, orange dashed lines show the mean bootstrap estimate and green dotted lines show implementation error estimates from (7). The left column shows log-evidence calculations and the right column shows estimates of the mean of the parameter  $\theta_1$  for 2-dimensional Gaussian, Rastrigin, Rosenbrock and Gaussian shell likelihoods with uniform priors. Results for each `num_repeats` value were calculated using 500 nested sampling runs, each with 100 live points. In each case the mean calculation result for each estimator is very close to the correct value, and consequently the root-mean-squared error is very close to the standard deviation of results — we therefore do not show it in the plot.

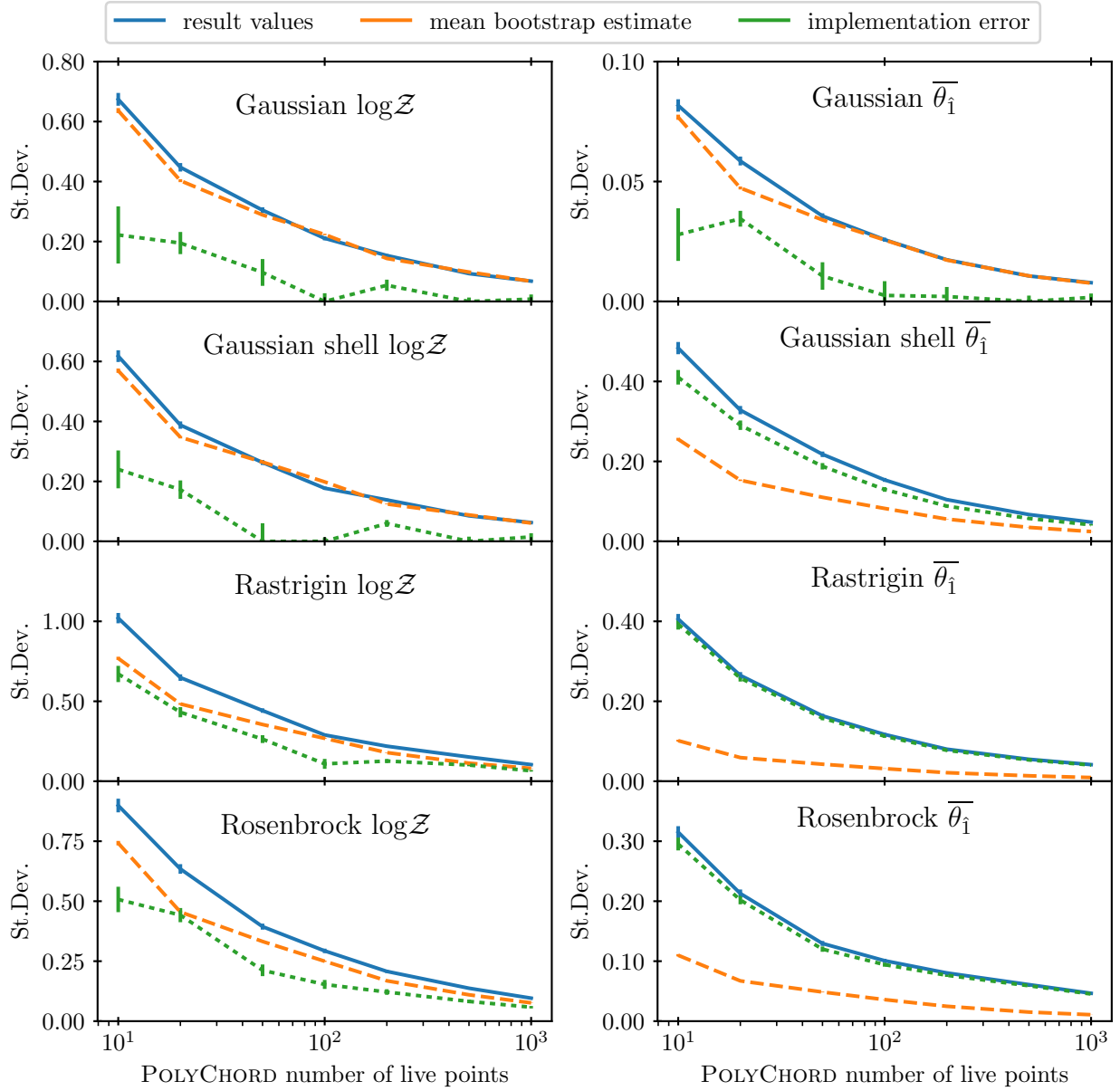


Figure 8: The effect of the number of live points on errors in POLYCHORD calculations: blue solid lines show the standard deviation of calculation results, orange dashed lines show the mean bootstrap estimate and green dotted lines show the error from implementation of the nested sampling algorithm inferred from (7). The left column shows log-evidence calculations and the right column shows estimates of the mean of the parameter  $\theta_1$  for 2-dimensional Gaussian, Rastrigin, Rosenbrock and Gaussian shell likelihoods with uniform priors. Results for each number of live points considered were calculated using 500 nested sampling runs with `num_repeats` = 5. In each case the mean calculation result for each estimator is very close to the correct value, and consequently the root-mean-squared error is very close to the standard deviation of results — we therefore do not show it in the plot.

nested sampling errors which do not account for implementation-specific effects may not be accurate.

Figures 7 and 8 also show that for each likelihood, log-evidence calculations have a lower fraction of their variation in results from implementation-specific effects than estimates of the mean of a parameter for the settings considered, in agreement with Figure 6. This is largely because the errors from the stochasticity of the nested sampling algorithm in evidence calculations are much larger than those in parameter estimations.

## 6 Diagnostic tests for when few runs are available

For computationally expensive problems there may not be enough nested sampling runs available to calculate the implementation-specific effects directly using the method described in the previous section. However, unless one has additional knowledge of the posterior distribution, it is impossible to tell *a priori* whether a single nested sampling run contains significant implementation-specific effects. In Sections 6.1 and 6.2 we therefore consider diagnostics which assess whether two nested sampling runs have consistently explored a parameter space while accounting for the stochastic nature of the nested sampling algorithm. If  $N > 2$  runs are available then  $\binom{N}{2}$  pairwise tests can be computed and their results combined for greater accuracy.

Assessing whether implementation-specific effects are present from two nested sampling runs without additional knowledge about the posterior is a very challenging problem: it is important to emphasise that these tests are merely heuristics and in general one cannot rule out the presence of modes or degeneracies with small volumes in parameter space which have been missed by both runs. Hogg & Foreman-Mackey (2017, Section 5) provide an interesting analogous discussion of the similarly heuristic nature of MCMC convergence tests. As a result, it is also useful also consider qualitative comparisons using diagnostic plots of the types shown in Section 4 and any problem-specific knowledge of what the results should be.

### 6.1 Testing for correlations between threads in two different runs

We now introduce a test to assess whether nested sampling software is consistently exploring a posterior by comparing the constituent threads (single live point runs) of two nested sampling runs. Each thread represents a valid independent nested sampling run and can be used to make posterior inferences about quantities such as the evidence and the mean and median of parameters. The actual values calculated from each thread will have large errors due their small number of samples, but this does not matter as we are only testing if the values obtained from the threads in each run are consistent with being drawn from the same distribution.

We propose applying the 2-sample Kolmogorov-Smirnov (KS) test (Massey 1951) to different runs' threads by using each thread to calculate an estimate of a scalar quantity of interest (such as parameter means or the Bayesian evidence  $\mathcal{Z}$ ) with the following procedure:



1. divide the first nested sampling run into its  $n_1$  constituent threads, and calculate an estimate of the quantity from each;
2. divide the second nested sampling run into its  $n_2$  constituent threads, and calculate an estimate of the quantity from each;
3. apply the 2-sample KS test to  $n_1$  and  $n_2$  values calculated from the first and second runs respectively.

As a test statistic for distributions  $p(x)$  and  $q(x)$ , the KS test uses the maximum distance between their cumulative distributions  $F_p(x)$  and  $F_q(x)$

$$D_{p,q} = \sup_x |F_p(x) - F_q(x)|, \quad (9)$$

where  $\sup$  is the supremum. If  $n_1$  and  $n_2$  samples from  $p(x)$  and  $q(x)$  respectively are used, the corresponding  $p$ -values are

$$\alpha = 2 \exp \left( -\frac{2n_1n_2}{n_1 + n_2} D_{p,q}^2 \right), \quad (10)$$

In this case the  $p$ -value produced represents the probability that the estimates from the two nested sampling runs are drawn from the same distribution. A  $p$ -value close to zero implies that the values obtained from the threads in the two runs are statistically inconsistent and hence that implementation-specific effects are present. This procedure can also be used with other distribution-free tests such as the 2-sample Anderson-Darling test as an alternative to the KS test.

Figure 9 shows distributions of  $p$ -values computed between pairs of nested sampling runs. For the Rastrigin and Rosenbrock likelihoods, the median  $p$ -values are close to zero meaning that implementation-specific effects are almost certainly present (in agreement with the results in Figure 6). With only two runs available one may only calculate one  $p$ -value for each quantity, but there are many quantities which can be tested; for example the Bayesian evidence and the mean, median, higher moments and confidence intervals on each parameter (although tests on functions of the same parameter will not be independent). As a result this test should give enough information to detect implementation-specific effects in the Rastrigin and Rosenbrock cases from only two runs. One could also test multiple quantities together using a multi-dimensional KS test, although this is computationally challenging — see Fasano & Franceschini (1987) for a more detailed discussion.

It is important to note that the KS test  $p$ -value only determines whether implementation-specific effects are present and does not provide information about the size of implementation error, which must be assessed to determine if they are problematic for a given use case.<sup>3</sup> This can be done with the help of bootstrap resamples, as discussed in the next section.

---

<sup>3</sup>In particular as the  $p$ -value is a measure of statistical significance, with enough data (threads) one can get a statistically significant detection of implementation-specific effects even if they are relatively small and/or not important for the practical problem being examined.

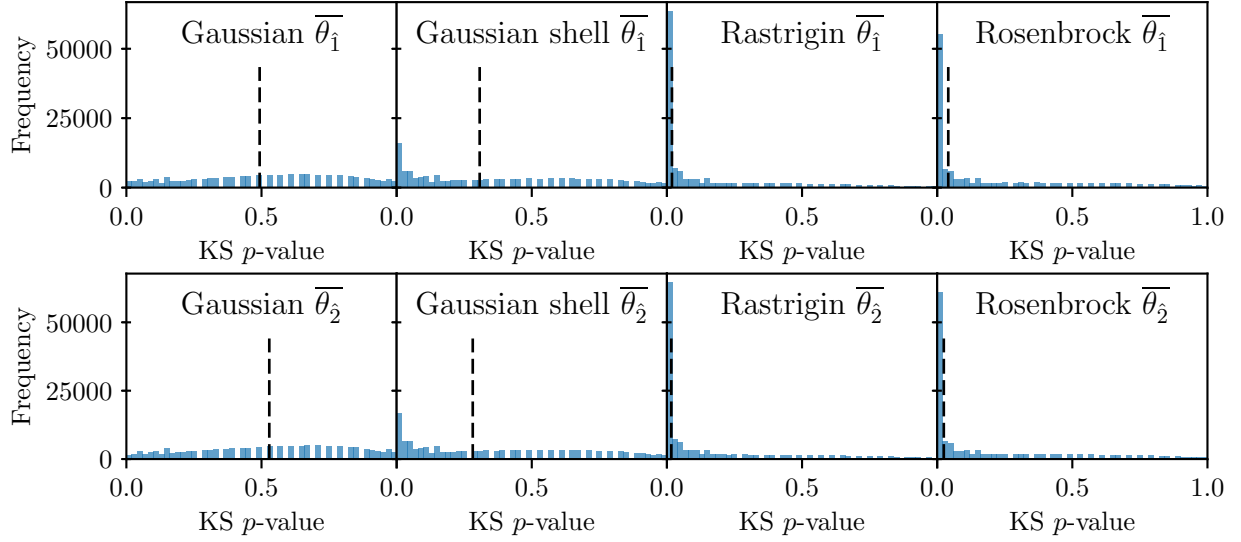


Figure 9: Distributions of KS test  $p$ -values from pairwise comparison of different runs' constituent threads. A  $p$ -value of 0 means the quantities calculated from threads in the two runs are from different distributions, meaning the threads within each run are correlated with each other and implementation-specific effects are present. The black dashed line shows the median  $p$ -value for each plot. The top and bottom rows of plots use distributions of estimates of the means of the parameters  $\theta_1$  and  $\theta_2$  from each thread. The nested sampling runs are the same ones that were used for Figure 6 — the 500 runs allow  $\binom{500}{2} = 124,750$  pairwise statistics to be computed.

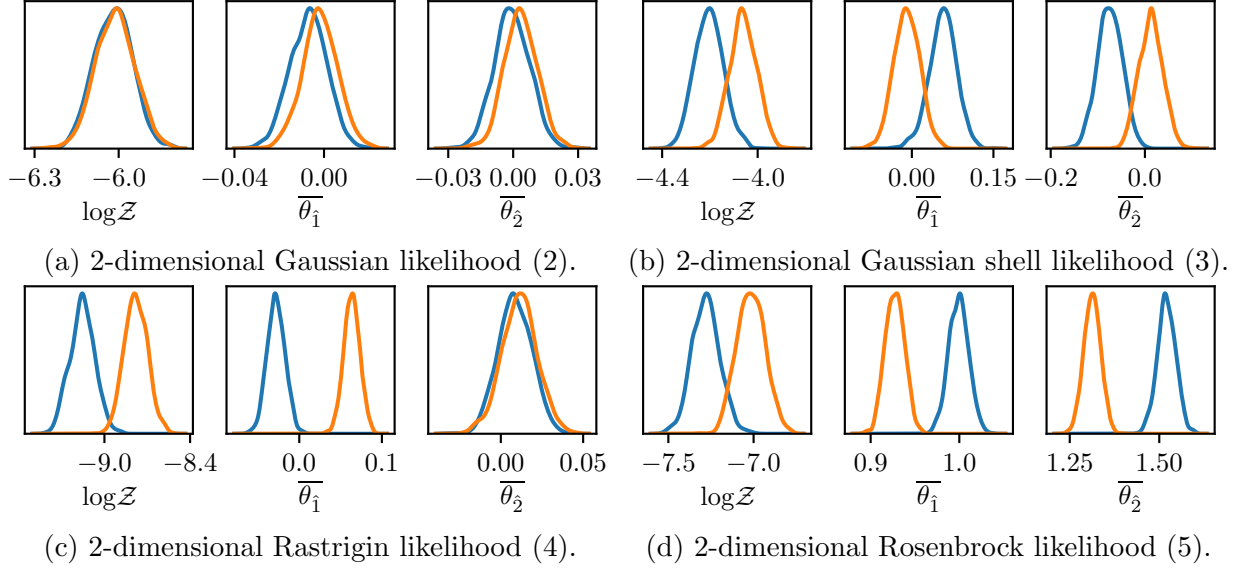


Figure 10: Plots of the sampling errors distribution calculated from bootstrap resampling threads for different quantities. Each plot shows 2 nested sampling runs (represented by different line colors), each with 1000 live points and `num_repeats` = 5. The kernel density estimation of the posterior distributions use a Gaussian kernel with the bandwidth selected using Scott’s rule (Scott 2015).

## 6.2 Distributions of sampling errors from bootstrap resamples

Our second diagnostic assesses whether calculations of scalar quantities from the two different runs differ by more than would be expected given the estimated uncertainties from the intrinsic stochasticity of the nested sampling algorithm. These uncertainty distributions can be calculated from bootstrap resamples using the method described in Higson et al. (2017b), and are illustrated in Figures 10a to 10d. This has some similarities with Figures 3a to 3d but differs in that, in order to more easily quantify the comparison between runs, we are now considering only errors on single numbers rather than on whole posterior distributions.

Whether the spread of results is explained by the bootstrap error distributions can be assessed qualitatively, or may be quantified by calculating measures of the statistical distance between the distributions. As with the comparisons of threads in Section 6.1 it may be hard to draw conclusions from any one quantity, but the two runs can be compared using estimates of the Bayesian evidence, the means, higher moments and credible intervals of parameters (although comparisons of functions of the same parameter will not be independent). We find the best distance measure is again the KS statistic (9); this constitutes a metric as it is non-negative, zero if and only if the distributions are equal, is symmetric and satisfies the triangle inequality. It is also easy to interpret, with a value of 1 meaning the distributions are the same and a value of 0 meaning they do not overlap. Alternative distance measures are discussed in Section A of the supplementary material.

Distributions of KS statistics calculated from bootstrap error distributions are shown in Figure 11. These distributions show that the median statistical distance between the

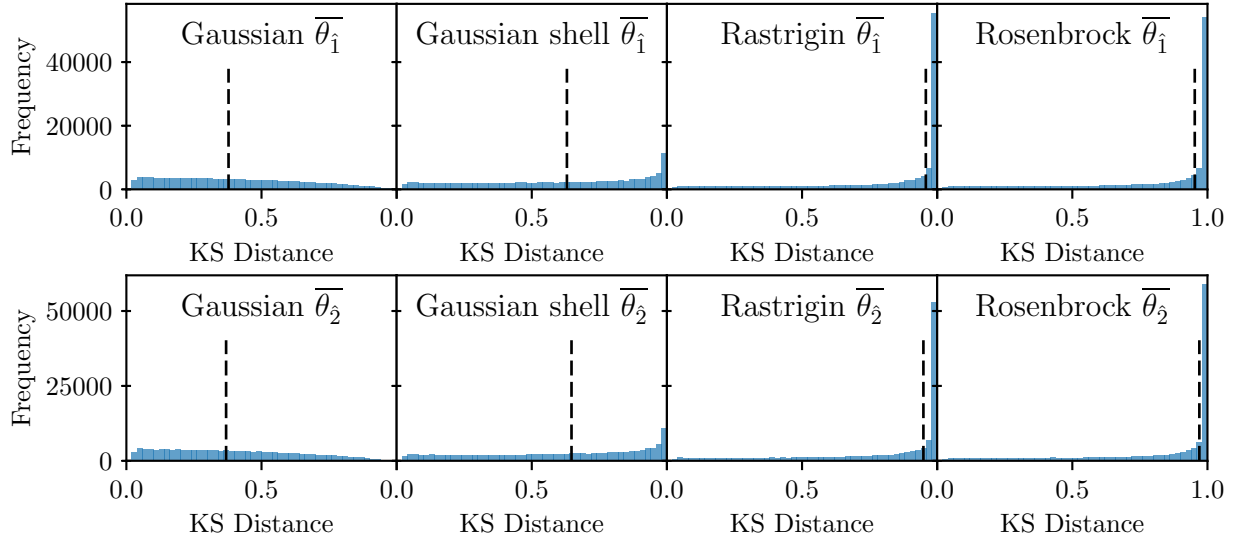


Figure 11: Distributions of KS statistical distances (KS statistics) (9) from pairwise comparison of different runs' bootstrap error distributions. A KS statistic of close to 1 means there is little overlap between the distributions, implying that the differences in the runs' values cannot be explained by the intrinsic stochasticity of the nested sampling algorithm and that implementation-specific effects are present. The black dashed line shows the median KS distance for each plot. The bootstrap error distributions on estimates of the mean of the parameters  $\theta_1$  and  $\theta_2$  for each run are used in the top and bottom rows respectively. The nested sampling runs are the same ones that were used for Figure 6; 500 runs allow  $\binom{500}{2} = 124,750$  pairwise statistics to be computed.

bootstrap uncertainty distributions for the Rastrigin and Rosenbrock cases is close to 1. There is therefore little overlap between the distributions and implementation-specific effects are likely present. These distance measures are more difficult to interpret than the  $p$ -values in Section 6.1, but have the advantage that together with plots like Figure 10 they contain information about the size of any implementation-specific effects as well as testing if implementation-specific effects are present. In this context, the KS statistic values are simply used as a distance measure and cannot be interpreted as  $p$ -values; even without implementation-specific effects, nested sampling runs will differ due to the stochasticity of the algorithm and so bootstrap resamples of different runs are always drawn from different distributions.

## 7 Summary

In this paper we introduced diagnostic tests for nested sampling software, which uses numerically techniques to generate approximately uncorrelated samples within hard likelihood constraints. As a result, for challenging problems — such as those with multimodal or degenerate posteriors — additional errors may be produced which would be present if the nested sampling algorithm was performed perfectly (we term these implementation-specific effects). Detecting the presence of significant implementation-specific effects is of great importance for software users as it determines whether results and estimates of uncertainties can be relied upon, and if the settings should be changed.

We suggested two new diagnostic diagrams for visualising nested sampling results and uncertainties and for comparing nested sampling runs; these are shown in Figures 3 to 5. Section 5 introduced a quantitative measure of implementation-specific effects, which can be used to estimate them directly if  $\sim 8$  or more nested sampling runs are available, and empirically tested the effects of nested sampling software settings on such errors. Finally, in Section 6, we provided two diagnostic tests which allow practitioners to detect implementation-specific effects using few as two nested sampling runs:

1. correlations within runs can be tested by dividing them into their constituent threads and using the Kolmogorov-Smirnov test as described in Section 6.1;
2. the consistency of the variation of results with estimates of the error from the intrinsic stochasticity of the nested sampling algorithm can be checked with statistical distance measures as described in Section 6.2.

When more than two runs are available, the results of these diagnostics on pairs of runs can be combined for greater accuracy.

We have written a publicly available software package **nestcheck** which performs diagnostics on input nested sampling runs and produces plots like Figures 3 to 5. It is compatible with results from MULTINEST v3.11 and POLYCHORD v1.13 (the latest versions at the time of writing), and can be downloaded at <https://github.com/ejhigson/nestcheck>.

## SUPPLEMENTARY MATERIAL

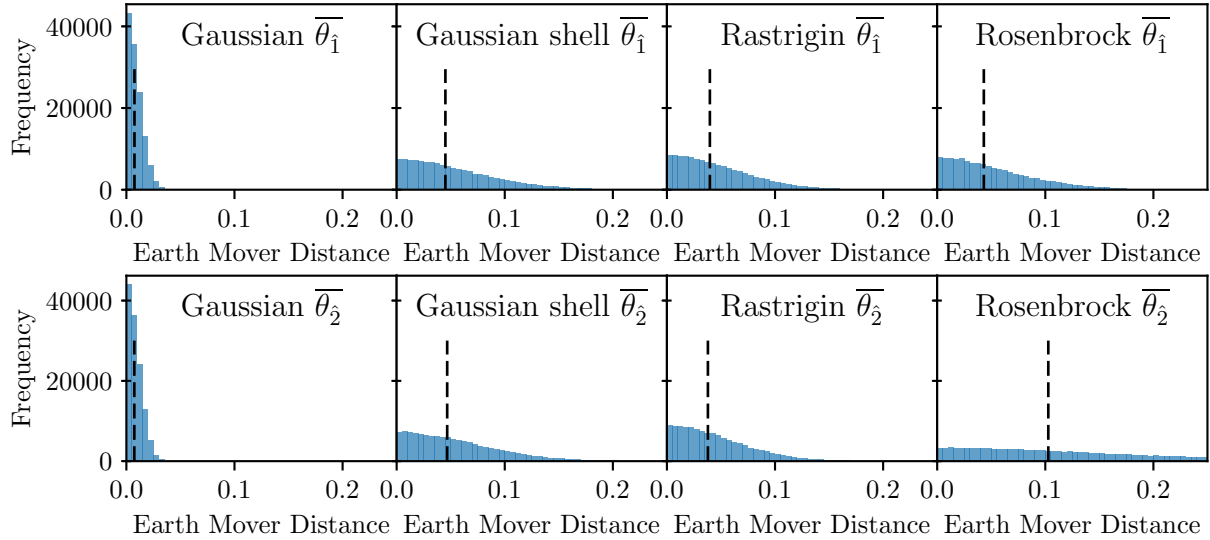


Figure 12: As for Figure 11 but using the earth mover’s distance instead of the KS statistic.

## A Other distance measures

The bootstrap error distributions diagnostics discussed in Section 6.2 could use a different measure of statistical distance instead of the KS statistic. However, as the distance must be computed from distributions of samples which may cover very different regions, measures which require the distributions have the same support such as the symmetrised Kullback-Leibler divergence cannot be computed robustly.

Two possible alternatives to the KS statistic are the energy distance (Székely & Rizzo 2013)

$$D_{p,q} = \left( \frac{1}{2} \int_{-\infty}^{\infty} (F_p(x) - F_q(x))^2 dx \right)^{\frac{1}{2}}, \quad (11)$$

and the earth mover’s distance (first Wasserstein distance), which is informally the minimum cost (defined as area multiplied by distance) required to move one distribution probability density function onto the other (for a more detailed discussion see Ramdas et al. 2017). Histograms of the pairwise distance estimate distribution from bootstrap error estimates on different runs are shown in Figures 11 and 12; in each case larger distances are associated with greater implementation-specific effects. We prefer the KS statistic as it is more sensitive than these measures, with more easily interpretable numerical values.

## B Numerical results tables

Tables 1 to 4 given numerical results for the nested sampling runs plotted in Figure 6.

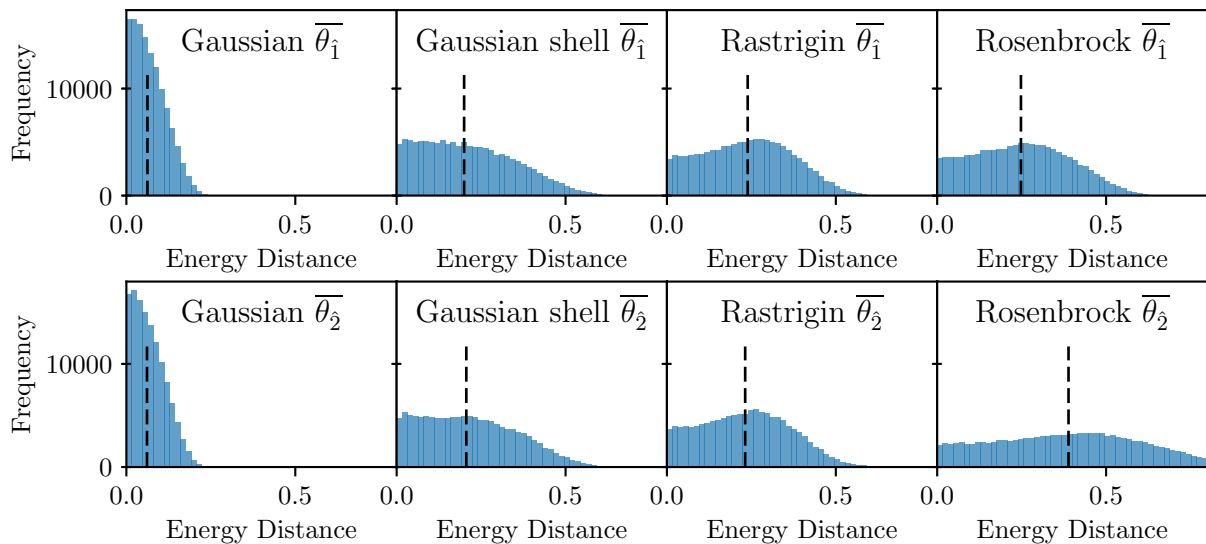


Figure 13: As for Figure 11 but using the energy distance instead of the KS statistic.

	$\log \mathcal{Z}$	$\overline{\theta_1}$	$\overline{\theta_2}$	$ \overline{\theta} $	$\overline{\theta_1^2}$
Correct Result	-5.9915	0.0000	0.0000	0.6267	0.2500
Mean Calculation Result	-5.969(9)	-0.001(1)	-0.000(1)	0.624(1)	0.2483(9)
Values St.Dev.	0.211(7)	0.0258(8)	0.0246(8)	0.0228(7)	0.0193(6)
Values RMSE	0.212(6)	0.0258(8)	0.0246(8)	0.0229(7)	0.0194(6)
Bootstrap St.Dev.	0.214(1)	0.0251(1)	0.0249(1)	0.0219(1)	0.0183(1)
Implementation St.Dev.	0.00(5)	0.006(5)	0.000(5)	0.006(4)	0.006(3)
Imp St.Dev. / Val St.Dev.	0.0(2)	0.2(2)	0.0(2)	0.3(2)	0.3(1)

Table 1: Calculation error results for the 500 nested sampling runs with a Gaussian likelihood shown in Figure 6. The first row shows the correct result for each estimator; these are calculated analytically or, where this is not possible, by numerical integration (which can be done accurately in these 2-dimensional cases). In every case the correct result is close to the mean calculation value shown in the second row — implying that despite any implementation-specific effects the nested sampling calculations are approximately unbiased. As a result the standard deviation of results and root-mean-squared error shown in the third and fourth row are very similar and we are justified in using the standard deviation of repeated results to analyse implementation-specific effects. The next three rows show the bootstrap error estimate, implementation error estimate (7) and the ratio of the implementation estimate to the standard deviation of results. Columns show results for the log-evidence, the mean of the two parameters, the mean radial coordinate and the second moment of  $\theta_1$ . Numbers in parentheses show the  $1\sigma$  numerical uncertainty on the final digit.

	$\log \mathcal{Z}$	$\overline{\theta_1}$	$\overline{\theta_2}$	$ \overline{\theta} $	$\overline{\theta_1^2}$
Correct Result	-4.1509	0.0000	0.0000	2.0200	2.0600
Mean Calculation Result	-4.134(8)	0.000(7)	0.007(7)	2.0198(5)	2.057(6)
Values St.Dev.	0.177(6)	0.154(5)	0.149(5)	0.0113(4)	0.127(4)
Values RMSE	0.178(6)	0.154(5)	0.149(4)	0.0113(3)	0.127(4)
Bootstrap St.Dev.	0.1938(9)	0.0808(4)	0.0813(4)	0.01112(5)	0.0872(4)
Implementation St.Dev.	0.00(1)	0.131(6)	0.124(6)	0.002(2)	0.093(6)
Imp St.Dev. / Val St.Dev.	0.00(9)	0.85(1)	0.84(1)	0.2(2)	0.73(2)

Table 2: As in Table 1 but for calculations using the Gaussian shell likelihood (3).

	$\log \mathcal{Z}$	$\overline{\theta_1}$	$\overline{\theta_2}$	$ \overline{\theta} $	$\overline{\theta_1^2}$
Correct Result	-8.9606	0.0000	0.0000	0.8189	0.4990
Mean Calculation Result	-8.90(1)	0.005(5)	-0.006(5)	0.832(5)	0.504(4)
Values St.Dev.	0.289(9)	0.117(4)	0.114(4)	0.109(3)	0.097(3)
Values RMSE	0.29(1)	0.117(4)	0.114(4)	0.110(3)	0.097(4)
Bootstrap St.Dev.	0.263(1)	0.0312(2)	0.0314(2)	0.0335(2)	0.0331(2)
Implementation St.Dev.	0.12(2)	0.113(4)	0.109(4)	0.104(4)	0.091(3)
Imp St.Dev. / Val St.Dev.	0.42(7)	0.964(2)	0.961(3)	0.952(3)	0.940(4)

Table 3: As in Table 1 but for calculations using the Rastrigin likelihood (4).

	$\log \mathcal{Z}$	$\overline{\theta_1}$	$\overline{\theta_2}$	$ \overline{\theta} $	$\overline{\theta_1^2}$
Correct Result	-7.1504	0.9974	1.4890	1.8630	1.4890
Mean Calculation Result	-7.10(1)	0.971(5)	1.45(1)	1.82(1)	1.45(1)
Values St.Dev.	0.293(9)	0.101(3)	0.219(7)	0.231(7)	0.219(7)
Values RMSE	0.296(9)	0.104(3)	0.222(7)	0.234(7)	0.221(7)
Bootstrap St.Dev.	0.247(1)	0.0353(2)	0.0783(5)	0.0823(5)	0.0782(5)
Implementation St.Dev.	0.16(2)	0.094(3)	0.204(7)	0.216(8)	0.204(7)
Imp St.Dev. / Val St.Dev.	0.54(4)	0.937(4)	0.934(4)	0.934(4)	0.934(4)

Table 4: As in Table 1 but for calculations using the Rosenbrock likelihood (5).



## References

- Allison, R. & Dunkley, J. (2014), ‘Comparison of sampling techniques for bayesian parameter estimation’, *Monthly Notices of the Royal Astronomical Society* **437**(4), 3918–3928.
- Buchner, J. (2016), ‘A statistical test for Nested Sampling algorithms’, *Statistics and Computing* **26**(1-2), 383–392.
- Fasano, G. & Franceschini, A. (1987), ‘A multidimensional version of the Kolmogorov-Smirnov test’, *Monthly Notices of the Royal ...* **225**, 155–170.  
**URL:** <http://adsabs.harvard.edu/full/1987mnras.225..155f>
- Feroz, F. & Hobson, M. P. (2008), ‘Multimodal nested sampling: An efficient and robust alternative to Markov Chain Monte Carlo methods for astronomical data analyses’, *Monthly Notices of the Royal Astronomical Society* **384**(2), 449–463.
- Feroz, F., Hobson, M. P. & Bridges, M. (2008), ‘MultiNest: an efficient and robust Bayesian inference tool for cosmology and particle physics’, *Monthly Notices of the Royal Astronomical Society* **398**(4), 1601–1614.  
**URL:** <http://dx.doi.org/10.1111/j.1365-2966.2009.14548.x>
- Feroz, F., Hobson, M. P., Cameron, E. & Pettitt, A. N. (2013), ‘Importance Nested Sampling and the MultiNest Algorithm’, *preprint (arXiv:1306.2144)*.
- Foreman-Mackey, D. (2016), ‘corner.py: Scatterplot matrices in Python’, *The Journal of Open Source Software* **1**(2), 9–10.  
**URL:** <http://joss.theoj.org/papers/10.21105/joss.00024>
- Handley, W. J., Hobson, M. P. & Lasenby, A. N. (2015a), ‘PolyChord: Nested sampling for cosmology’, *Monthly Notices of the Royal Astronomical Society: Letters* **450**(1), L61–L65.
- Handley, W. J., Hobson, M. P. & Lasenby, A. N. (2015b), ‘PolyChord: next-generation nested sampling’, *Monthly Notices of the Royal Astronomical Society* **15**, 1–15.
- Higson, E., Handley, W., Hobson, M. & Lasenby, A. (2017a), ‘Dynamic nested sampling : an improved algorithm for parameter estimation and evidence calculation’, *arXiv preprint* (0).
- Higson, E., Handley, W., Hobson, M. & Lasenby, A. (2017b), ‘Sampling errors in nested sampling parameter estimation’, *Bayesian Analysis*.  
**URL:** <https://doi.org/10.1214/17-BA1075>
- Hogg, D. W. & Foreman-Mackey, D. (2017), ‘Data analysis recipes: Using Markov Chain Monte Carlo’.  
**URL:** <http://arxiv.org/abs/1710.06068>
- Keeton, C. R. (2011), ‘On statistical uncertainty in nested sampling’, *Monthly Notices of the Royal Astronomical Society* **414**(2), 1418–1426.

- Lewis, A. (2015), ‘GetDist : Kernel Density Estimation’, pp. 1–11.
- Massey, F. J. (1951), ‘The Kolmogorov-Smirnov Test for Goodness of Fit’, *Journal of the American Statistical Association* **46**(253), 68– 78.  
**URL:** <http://www.jstor.org/stable/2280095>
- Murray, I. (2007), Advances in Markov chain Monte Carlo methods, PhD thesis, University College London.  
**URL:** <http://discovery.ucl.ac.uk/182011/>
- Ramdas, A., Trillos, N. G. & Cuturi, M. (2017), ‘On wasserstein two-sample testing and related families of nonparametric tests’, *Entropy* **19**(2), 1–15.
- Scott, D. W. (2015), *Multivariate Density Estimation: Theory, Practice, and Visualization*.  
**URL:** <https://books.google.com.tr/books?id=XZ03BwAAQBAJ%0Apapers3://publication/uuid/CA73D1A68-4B3A-9C64-2996A05893D2>
- Skilling, J. (2006), ‘Nested sampling for general Bayesian computation’, *Bayesian Analysis* **1**(4), 833–860.
- Székely, G. J. & Rizzo, M. L. (2013), ‘Energy statistics: A class of statistics based on distances’.